Separation Science and Technology
Publication details, including instructions for authors and subscription information:
http://www.informaworld.com/smpp/title~content=t713708471

Concentration Profiles in Hollow-Fiber Dialyzers

John A. Baker[a]; James O. Osburn[a]; Richard L. Lawton[b]
[a] DEPARTMENT OF CHEMICAL AND MATERIALS, ENGINEERING UNIVERSITY OF IOWA IOWA CITY, IOWA [b] DEPARTMENT OF SURGERY, UNIVERSITY OF IOWA IOWA CITY, IOWA

To cite this Article Baker, John A. , Osburn, James O. and Lawton, Richard L.(1974) 'Concentration Profiles in Hollow-Fiber Dialyzers', Separation Science and Technology, 9: 5, 411 — 422
To link to this Article: DOI: 10.1080/00372367408056076
URL: http://dx.doi.org/10.1080/00372367408056076

SEPARATION SCIENCE, 9(5), pp. 411–422, 1974

Concentration Profiles in Hollow-Fiber Dialyzers

JOHN A. BAKER and JAMES O. OSBURN

DEPARTMENT OF CHEMICAL AND MATERIALS ENGINEERING
UNIVERSITY OF IOWA
IOWA CITY, IOWA 52242

RICHARD L. LAWTON

DEPARTMENT OF SURGERY
UNIVERSITY OF IOWA
IOWA CITY, IOWA 52242

Abstract

Concentration profiles in hollow-fiber dialyzers have been determined experimentally by the use of a hollow fiber dialysis cascade employing aqueous salt and urea solutions. A mathematical model has also been developed to predict radial and axial concentration profiles for co- and counter-current operation. The experimental and predicted results are compared.

INTRODUCTION

The need for compact and disposable hemodialyzers has led to the development of dialyzers composed of bundles of very small diameter (i.d. = 240 μ) hollow fibers made of regenerated cellulose. Such dialyzers have the advantage of reducing the blood-side diffusive resistance, thus providing improved separation for blood purification. The advantages of hollow-fiber hemodialyzers have been well described elsewhere (*1–3*).

In this study several Dow-Cordis (The Cordis Corp., Miami, Florida) hollow-fiber artificial kidneys were connected in series to determine length–concentration profiles during dialysis of aqueous salt and urea solutions. A mathematical model was developed and the calculated profiles

derived from this model compared to the experimental results. Radial and axial concentration gradients may be predicted for both co- and countercurrent operation from the model. These concentration profiles are useful in determining the mass transfer coefficients for both the blood and dialysate-side of the hollow-fiber membrane.

Experimental

The hollow-fiber dialysis cascade is shown in Fig. 1. The Dow-Cordis artificial kidney is designed so that the blood-side fluid flows through the inside of the hollow fibers. Characteristics of the Dow-Cordis kidney are given in Table 1. Connections between units were made with Tygon tubing. Mercury manometers and rotameters were placed in the inlet fluid lines to monitor pressures and flow rates. Dilute aqueous solutions of sodium chloride and urea were used as blood-side fluids while distilled water was used as the dialysate-side fluid. Solutions were contained in 5 gal carboys and fed to the unit by pulsatile pumps. Recycle lines from the pump discharge lines back to the carboys allowed for any combination of flow rates to be obtained. The concentration of chloride ion used in the feed stream was 0.0296 *M* and for urea solutions the concentration used was 50 mg-% blood urea nitrogen (BUN).

From each fluid stream of the cascade six samples were taken for analysis, sample ports being located after each hollow-fiber unit. Sample ports consisted of plastic tees inserted into the Tygon tubing connecting the

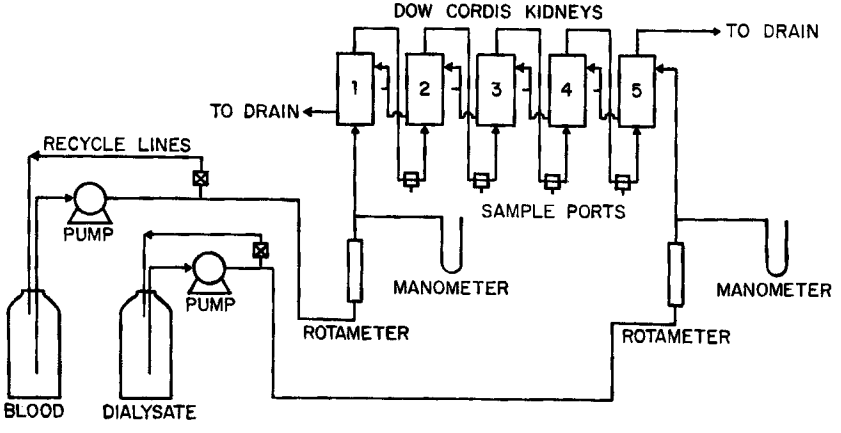

FIG. 1. Hollow-fiber dialysis cascade.

individual units, with the sample taken by releasing a pinch clamp on a drain line. Samples were taken after steady-state conditions had been obtained, usually 15 to 20 min after flow rates and pressures had been set.

Analysis for chloride ion was made by the Mohr titrametric method. Urea analyses were made by use of a Technicon Auto-Analyzer. The sodium chloride samples were taken at a run temperature of 23°C; the urea samples were taken at a run temperature of 30°C.

For the two cocurrent runs a sodium chloride solution (0.0296 *M*) was used as the blood-side fluid. The flow rates for the two runs were: 150 ml/min on the blood-side and 255 ml/min on the dialysate-side; and for the second run, 250 ml/min on the blood-side and 435 ml/min on the dialysate-side. For the lower flow rate the average transmembrane pressure was 32 Torrs; for the higher flow rate the average transmembrane pressure was 115 Torrs. Ambient temperature for the cocurrent NaCl run was 23°C; ambient temperature for the countercurrent urea run was 30°C.

TABLE 1

Characteristics of the Dow-Cordis Model 3 Hollow-Fiber Hemodialyzer

Description: A hollow-fiber bundle contained in a cylindrical plastic shell, the hollow fibers being potted in silicone rubber.
Dimensions: 21.6 cm long by 7 cm in diameter.
Membrane: 11,000 hollow fibers made of regenerated cellulose. Effective length: 13.5 cm. Inside diameter: 225 μ. Wall thickness: 30 μ. Effective surface area: 1 m^2.
Priming volumes: Blood side: 95 ml. Dialysate side: 100 ml.
Flow resistance: 0.175 Torr/(ml)(min) for blood in blood-side compartment
Ultrafiltration rate: 135 ml/(hr)(Torr)

Mathematical Model

A mathematical model has been developed to simulate the concentration profiles occurring in the hollow-fiber dialysis cascade. This model simulates a hypothetical average hollow fiber with surrounding annulus. This average fiber and annulus is assumed to represent the cascade as a whole. The model is based on differential equations derived from mass balances, and these equations may be solved by implicit finite difference equation methods.

From a material balance using convective and diffusive equations, the following differential equation can be derived in cylindrical coordinates (*4*)

$$\left[1 - \left(\frac{r}{R}\right)^2\right] u \frac{\partial c}{\partial z} = \left(\frac{\partial^2 c}{\partial r^2} + \frac{1}{r}\frac{\partial c}{\partial r}\right) \tag{1}$$

The assumptions which are made in the derivation and use of this equation are:

(1) Diffusion is important only in the radial direction.
(2) There is no fluid convection radially.
(3) Laminar velocity profiles exist inside the tube and annulus.
(4) Diffusivity is constant.
(5) Entrance effects are neglected.

To nondimensionalize the differential equation, the following substitutions were made: $X = c/c_0$, $\lambda = z/L$, and $u = r/R$, and therefore for the blood-side

$$(1 - u^2)\frac{\partial X}{\partial \lambda} = \alpha\left(\frac{\partial^2 X}{\partial u^2} + \frac{1}{u}\frac{\partial X}{\partial u}\right) \tag{2}$$

where $\alpha = LD/R^2 u_1$ and u_1 is the blood-side velocity.

By the use of subscripts (i for the radial dimension, j for the axial dimension) the differential equation may be written as a set of linear algebraic equations amenable to solution by matrix methods. For instance, the derivatives of concentration with respect to radius and length may be written as

$$\frac{\partial^2 X}{\partial u^2} = \frac{1}{2h^2}[(X_{i+1,j+1} - X_{i,j+1} + X_{i-1,j+1}) + (X_{i+1,j} - X_{i,j} + X_{i-1,j})] \tag{3}$$

$$\frac{1}{u}\frac{\partial X}{\partial u} = \frac{1}{4u_i h}[(X_{i+1,j+1} - X_{i-1,j+1}) + (X_{i+1,j} - X_{i-1,j})] \tag{4}$$

$$(1 - u^2)\frac{\partial X}{\partial \lambda} = (1 - u_i^2)(X_{i,j+1} - X_{i,j})/k \tag{5}$$

The subscripted concentrations are those at various nodes in the cross section of a hollow fiber and annulus surrounding the fiber. This subscripting is demonstrated in Fig. 2 where at a given axial position the radial subscripts are indicated.

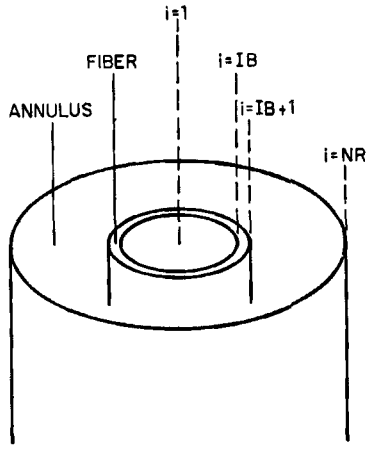

FIG. 2. Diagram of subscripting in dialysis cascade model.

By substitution of Eq. (3), (4), and (5) into Eq. (2), a primary difference equation for the tube side is obtained. The following boundary and initial conditions are used to solve the equation:

(1) At $i = 1$, the tube centerline, there is no flux across the centerline, therefore $\partial c/\partial r = 0$.

(2) At $i = IB$ and at $i = IB + 1$, the flux is proportional to the concentration difference across the membrane or $D(\partial c/\partial r) = -P\Delta c$, where P is a proportionality constant dependent upon permeability characteristics of the membrane.

(3) At $i = NR$, there is no flux across the annulus boundary or $\partial c/\partial r = 0$.

(4) Radial concentrations across the inlet of the tube and annulus are initialized to appropriate values depending upon the mode of operation

For the annulus side (dialysate side), Eq. (2) must be modified to account for the different velocity on that side, and a new variable, β, analogous to α, may be used: $\beta = LD/R^2u_2$, where u_2 is the dialysate-side velocity.

The differential equation for the annulus side employs the laminar velocity profile for an annulus and the differential equation becomes

$$[1 - u^2 + [(1 - K^2)/\ln(1/K)](\ln u)]\frac{\partial X}{\partial \lambda} = \beta\left(\frac{\partial^2 X}{\partial u^2} + \frac{1}{u}\frac{\partial X}{\partial u}\right) \qquad (6)$$

where K is the ratio of the inner to the outer annular radii. This equation may then be reduced to finite difference representation as before.

For any particular axial position the model generates a set of six linear equations that are used to calculate dimensionless concentrations based on concentrations found at the previous axial position. The initialization of the entrance concentrations begins the generation of the algebraic coefficients. The method used to solve for these coefficients is the Thomas method (*4*), this being a specific solution for tridiagonal matrices such as the one generated by this model.

A computer program was written to predict concentration profiles by the use of the mathematical model. The program calculated point concentrations, and these were averaged across a radial section so that they could be compared to the experimental values. In Fig. 3 is shown a representation of a volume element and point concentrations from which an average concentration for the element may be determined.

An arithmetic average of the point concentrations approximates the mixing cup concentration. For a generalized volume the average concentration in this volume would be

$$\overline{C_{ij}} = \tfrac{1}{4}(C_{ij} + C_{i+1,j} + C_{i,j+1} + C_{i+1,j+1})$$

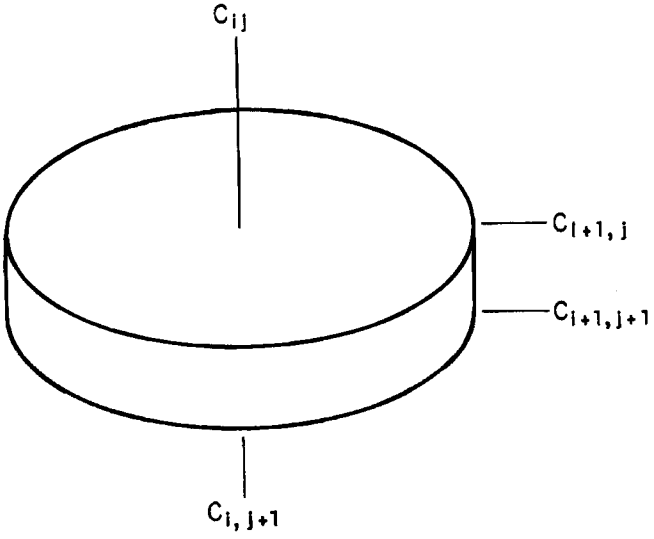

FIG. 3. Use of subscripts for calculating average concentrations.

These average concentrations may then be multiplied by the volume that they are associated with to give the number of moles of solute in that volume. This method of averaging is a good approximation because of the small volumes involved, the small changes in concentrations from one point to the next, and the approximately linear nature of the concentration profiles between the points.

The model was solved by use of an IBM 360 digital computer employing Fortran IV language.

RESULTS AND DISCUSSION

The mathematical model requires that operational data, dimensions of the hollow fibers and dialysis cell, diffusivity of solution components, and membrane permeabilities be supplied for the calculations. The diffusivity of sodium chloride for the concentration used at 23°C is 1.6×10^{-5} cm^2/sec (*5*); the diffusivity of urea in solution at 30°C is 1.5×10^{-5} cm^2/sec (*6*). Membrane permeabilities for urea were determined from the literature (*7*) for the two temperatures, and these were used in the calculations since the membrane permeabilities of sodium chloride and urea through regenerated cellulose membranes are nearly the same. In order to determine these permeabilities an effective diffusivity at the required temperature was found from the reported data, and from this the membrane permeabilities could be determined by the relationship

$$P = D_{eff}/t$$

where P is the membrane permeability (cm/sec), D_{eff} is the effective diffusivity of solute in the membrane (cm^2/sec), and t is the membrane thickness (cm). The values used for the effective diffusivity were 2.39×10^{-6} cm^2/sec at 30°C and 2.1×10^{-6} cm^2/sec at 23°C.

In Fig. 4 is shown a comparison of experimental and predicted results for cocurrent operation using a sodium chloride solution with two different arrangements of flow rates. The experimental results agree to within $\pm 1.3\%$ with the predicted results. This is good agreement considering the inherent errors in titrating, determining flow rates, and sampling, which could be as much as 5%. In Fig. 5 is shown the radial concentration profiles for the cocurrent case as predicted from the mathematical model. These profiles are very flat as would be expected from very small channels such as hollow fibers.

In Fig. 6 is shown a comparison of experimental and predicted results for countercurrent operation using a urea solution. Two flow schemes are

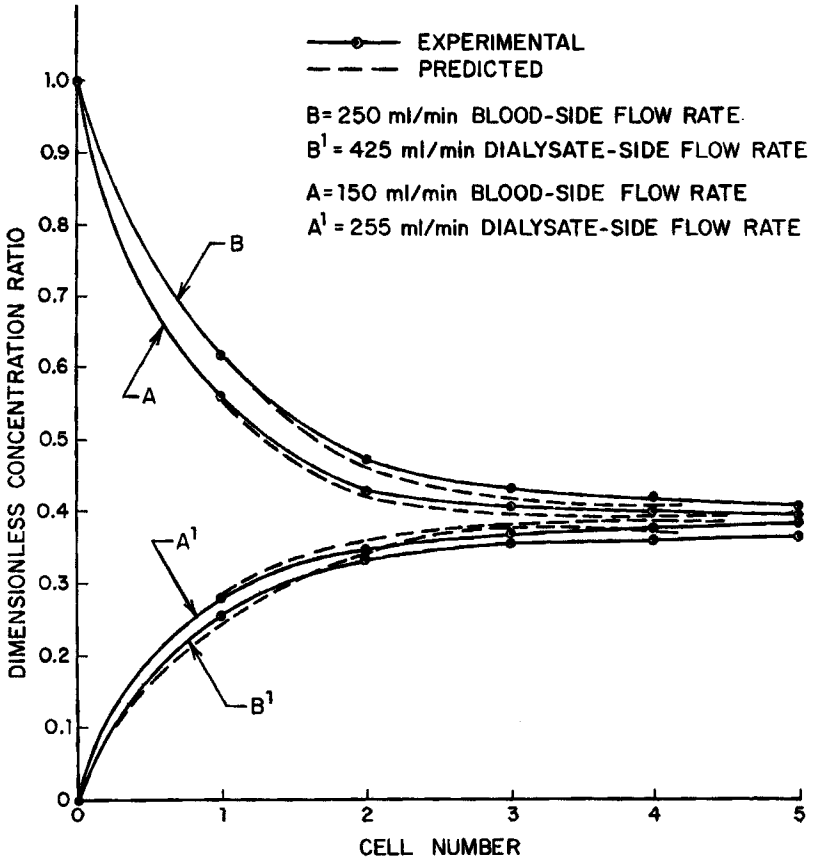

FIG. 4. Length–concentration profiles for cocurrent operation (feed solution, 0.0296 *M* NaCl).

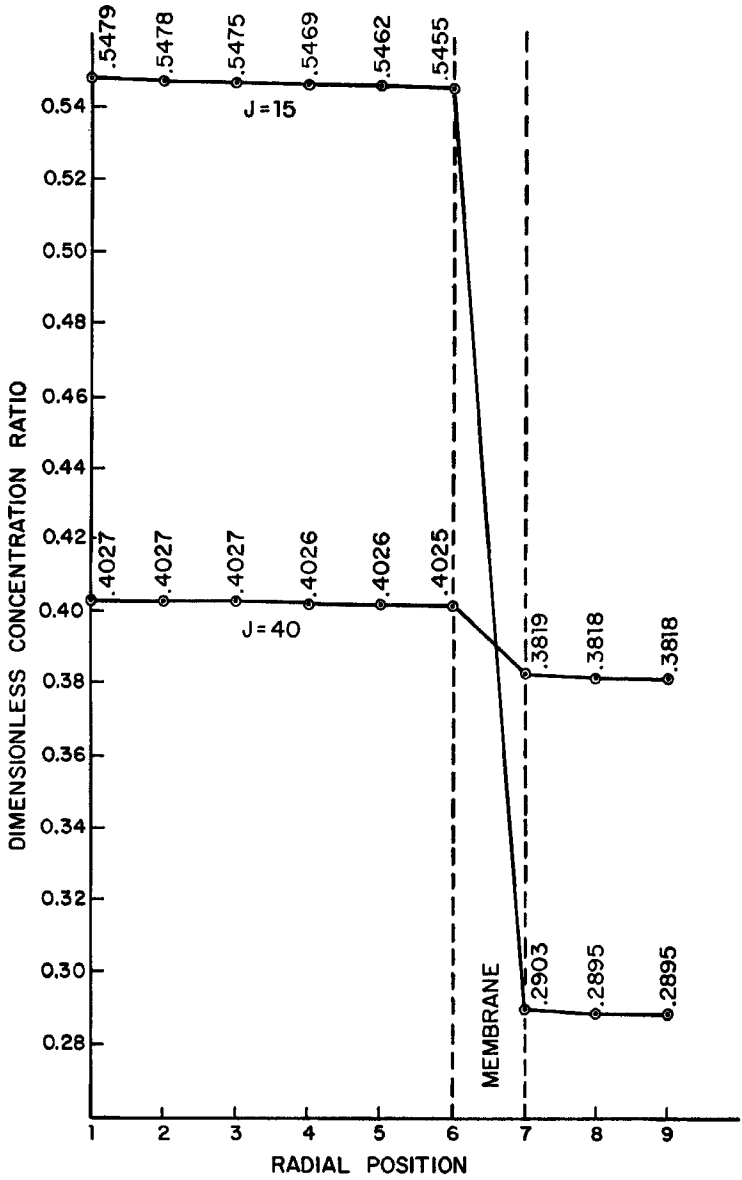

FIG. 5. Radial concentration profiles for cocurrent flow.

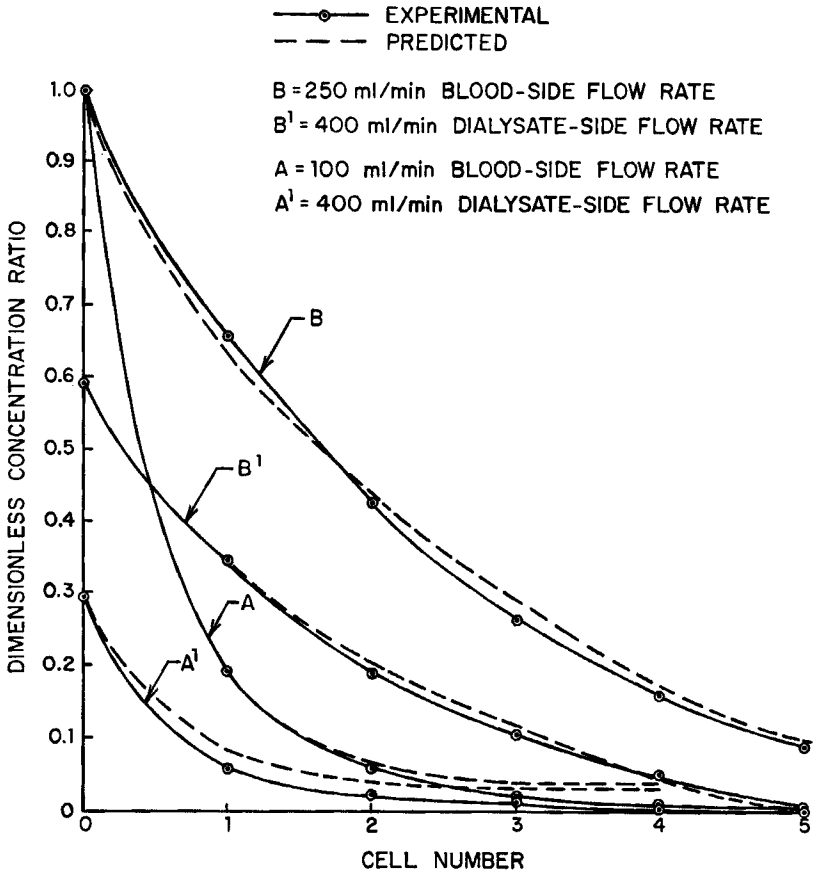

FIG. 6. Length–concentration profiles for countercurrent operation (feed solution, 50 mg% BUN).

shown for 100 ml/min blood-side and 400 ml/min dialysate-side flow rates and for 250 ml/min blood-side and 400 ml/min dialysate-side flow rates. For the 250–400 ml/min flow rates the average transmembrane pressure per cell was 25 Torrs (diaylsate-side pressure being higher) and the total net flow of ultrafiltrate into the blood side was 3.2 ml/min. The average deviation of the experimental results with respect to the predicted results for this case was $\pm 3.4\%$. About one-third of this error can be accounted for by ultrafiltration and the rest by errors mentioned above. For the 100–400 ml/min flow rates the average transmembrane pressure per cell was 72 Torrs and the total net flow of ultrafiltrate into the blood side was 9 ml/min. Since this represents a 9% error in the blood-side flow rate, one would expect a displacement of the experimental results as compared to the predicted results. This is noticed in Fig. 6 where a discrepancy for the higher cell numbers is noticeable.

SYMBOLS

c	concentration, moles/liter
D	diffusivity, cm^2/sec
h	radial spacing factor
i	radial node subscript
j	axial node subscript
K	ratio of inner to outer annular radii
k	axial spacing factor
L	total length of cascade fibers, cm
P	permeability constant, cm/sec
R	radius of hypothetical annulus surrounding fiber, cm
r	radial dimension, cm
u	dimensionless radial position
u_1	maximum velocity, blood-side, cm/sec
u_2	maximum velocity, dialysate-side, cm/sec
X	dimensionless concentration
z	axial dimension, cm

Greek Letters

α	LD/R^2u_1
λ	dimensionless axial position

REFERENCES

1. R. D. Stewart et al., *Trans. Amer. Soc. Artificial Internal Organs, 14,* 121 (1968).
2. R. D. Stewart et al., *Invest. Urology, 3,* 614 (1966).
3. F. Gotch et al., *Trans. Amer. Soc. Artificial Internal Organs, 15,* 87 (1969).
4. L. Lapidus, *Digital Computation for Chemical Engineers* McGraw-Hill, New York, 1962, p. 181.
5. R. C. Reid and K. Sherwood, *The Properties of Gases and Liquids,* 2nd ed., McGraw-Hill, New York, 1966, p. 563.
6. C. K. Colton et al., "Mass Transfer in Biological Systems," *Chem. Eng. Progr. Symp., 66,* 94 (1966).
7. A. L. Babb and P. C. Farrell, *J. Biomed. Mater. Res., 7,* 275 (1973).

Received by editor April 24, 1974